

MOX–Report No. 09/2013

**Patient-specific computational generation of the
Purkinje network driven by clinical measurements**

VERGARA, C.; PALAMARA, S.; CATANZARITI, D.;
PANGRAZZI, C.; NOBILE, F.; CENTONZE, M.; FAGGIANO,
E.; MAINES, M; QUARTERONI, A.; VERGARA, G.

MOX, Dipartimento di Matematica “F. Brioschi”
Politecnico di Milano, Via Bonardi 9 - 20133 Milano (Italy)

mox@mate.polimi.it

<http://mox.polimi.it>

PATIENT-SPECIFIC COMPUTATIONAL GENERATION OF THE PURKINJE NETWORK DRIVEN BY CLINICAL MEASUREMENTS

Christian Vergara, PhD, Dipartimento di Ingegneria, Università di Bergamo, Italy

Simone Palamara, MOX, Dipartimento di Matematica "Brioschi", Politecnico di Milano, Italy

Domenico Catanzariti, MD, Divisione di Cardiologia, Ospedale S. Maria del Carmine, Rovereto (TN), Italy

Cesarino Pangrazzi, Divisione di Cardiologia, Ospedale S. Maria del Carmine, Rovereto (TN) , Italy

Fabio Nobile, PhD, Dipartimento di Matematica "Brioschi", Politecnico di Milano, Italy, and MATHICSE-CSQI, École Polytechnique Fédérale de Lausanne, Switzerland

Maurizio Centonze, U.O. di Radiologia di Borgo-Pergine (Trento), Italy

Elena Faggiano, PhD, MOX, Dipartimento di Matematica "Brioschi", and LaBS, Dipartimento di Chimica, Materiali e Ingegneria Chimica, Politecnico di Milano, Italy

Massimiliano Maines, MD, Divisione di Cardiologia, Ospedale S. Maria del Carmine, Rovereto (TN), Italy

Alfio Quarteroni, MOX, Dipartimento di Matematica "Brioschi", Politecnico di Milano, and MATHICSE-CSQI, École Polytechnique Fédérale de Lausanne, Switzerland

Giuseppe Vergara, MD, Divisione di Cardiologia, Ospedale S. Maria del Carmine, Rovereto (TN), Italy

ABSTRACT

Rationale: The propagation of the electrical signal in the Purkinje network is the starting point of the activation of the muscular cells in the ventricle and of the contraction of the heart. Anomalous propagation in such a network can cause disorders such as ventricular fibrillation. In the computational models describing the electrical activity of the ventricle is therefore important to account for the Purkinje fibers.

Objective: Aim of this work is to apply to real cases a method for the generation of the Purkinje network driven by patient-specific measures of the activation on the endocardium, to compute the activation maps in the ventricle and to compare the accuracy with that of other strategies proposed so far in the literature.

Methods and Results: We consider MRI images of two patients and data of the activation times on the endocardium acquired by means of the EnSite NavX system. To generate the Purkinje network we use a fractal law driven by the measures. Our results show that for a normal activation our algorithm is able to reduce considerably the errors ($19.9\pm 5.3\%$ with our algorithm vs $33.9\pm 6.8\%$ with the best of the other strategies for patient 1, and $28.6\pm 6.0\%$ vs $63.9\pm 8.6\%$ for patient 2).

Conclusions: In this work we showed the reliability of the proposed method to generate a patient-specific Purkinje network. This allowed to improve the accuracy of computational models for the description of the electrical activation in the ventricle.

Keywords: Purkinje fibers, computational methods, activation times, Eikonal equation.

INTRODUCTION

Purkinje fibers (PF) represent the peripheral part of the cardiac conduction system (CCS) and are located in the inner ventricular walls of the heart, just beneath the endocardium. Their main role consists in providing rapid and coordinate activation of the ventricular myocardium¹, an essential feature for the correct pumping of the blood flow into the arteries. Anomalous propagation of the electrical signal can cause either electrical disorders such as ventricular fibrillation² or mechanical disorders such as ventricular dyssynchrony leading to heart failure^{3,4}. PF are electrically connected to the ventricular muscle only at certain insertion sites, called Purkinje muscle junctions (PMJ)⁵. From these sites the depolarization wave enters the heart wall, allowing the ventricular excitation and contraction through the activation of the cardiac muscle cells⁶.

The mathematical and computational models of cardiac electrophysiology allow to compute virtually the electrical activity in the ventricles⁷. The inclusion of CCS and in particular of the PF in such models has been seen to be essential to simulate not only healthy activations, but also pathological cases^{8,9}. However, radiological images do not allow to identify and reconstruct the PF.

In this work, we considered an approach based on the automatic generation of the PF by using the algorithm proposed in (Palamara, Vergara, Faggiano, Nobile, unpublished data, [2013]). This is based on a fractal law as proposed in^{10,11,12}. However, in these works the network generation has been obtained by considering only general anatomical information, whereas in our approach the construction of the network has also been driven by clinical patient-specific data of the activation times on the endocardium. At the best of the authors' knowledge, this is the first attempt to use clinical data for the explicit construction of the PF by means of computational models, allowing to obtain patient-specific Purkinje networks.

The purpose of this study is twofold: i) To show the applicability and reliability of our algorithm for the generation of patient-specific Purkinje networks in real cases; ii) To prove the essential role of PF in modeling the activation of the left ventricle.

METHODS

Patient-specific clinical measurements

Description of the patients and of the therapy

A 46-years-old and a 45-years-old individuals with Wolff-Parkinson-White (WPW) syndrome have been considered. The Electrocardiogram of both patients have revealed an anomalous electrical propagation within the left ventricle. Accordingly to the guidelines used in the laboratory, an electro-anatomical mapping of the left ventricle has been performed to localize the site of the anomalous pathway by using an EnSite NavX system (St Jude Medical), allowing to target and then interrupt the anomalous propagation with a catheter-based ablation procedure.

Acquisition of imaging data and reconstruction of the endocardium geometry

The day before the ablation therapy, the patients underwent Magnetic Resonance Imaging (MRI). Using a 1.5 Tesla MRI Unit (Magnetom Avanto, Siemens Medical Systems, Erlangen, Germany) and a 8 channel phased array torso coil, a non-contrast enhanced three-dimensional (3D) whole heart sequence, cardiac and respiratory gated, was performed using the following parameters: voxel resolution of 1.7x1.6x1.3 mm; TR (repetition Time)=269.46; TE (EchoTime)=1.46 ms; flip angle=90°; slice thickness=1.3 mm with 104 slices per single slab; acquisition matrix=256x173.

Then, the segmented images of the endocardium have been obtained by processing the MRI study using the EnSite Verismo™ Segmentation Tool (EnSite Verismo 2.0.1), which is based on a thresholding method. Later, the segmented images have been used to build the computational domains in view of the numerical simulations and have been imported into the EnSite NavX system to acquire the activation times on the endocardium.

Acquisition of electrical data

The Ensite NavX system is capable of accurately locating any electrode catheter within the 3D navigation field, allowing the reconstruction of the geometry of any cardiac chamber and providing accurate, real-time catheter navigation to guide mapping and ablation. The current version of Digital Image Fusion function of the EnSite NavX system allowed the segmented endocardium to be displayed side by side and synchronously rotated with the constructed geometry.

The system consists of three pairs of patches placed on the body surface which generate the 3D navigation field. Based on this, it is possible to measure the local voltage of any point of the endocardium and thus accurately compute the related electrical activation time.

In our cases, the left ventricular mapping to localize the anomalous pathway has been performed in the context of a bi-ventricular mapping, focusing in particular on the left posteroseptal region, for the first patient, and in the submitral region, focusing in particular on the left anterolateral region, for the second patient. In both the cases, in addition to the electro-catheters needed for the complete mapping, a 7 Fr deflectable electro-catheter has been inserted through the right femoral artery with a retrograde trans-aortic approach to obtain the left ventricular mapping and perform the ablation (Medtronic Enhancr II 5523/ Medtronic Conductr). The mapping procedure has been then performed also after the therapy to check the correct restoration of the normal propagation.

The study has been approved by the ethic committee of Azienda Provinciale per i Servizi Sanitari, Trento, Italy. The patients have been previously informed and gave their consent both for this invasive clinical procedure, needed to remove the anomalous activation and to restore the normal propagation and thus solving their clinical disorders, and for the successive mathematical elaborations.

Patient-specific generation of the Purkinje fibers network

The electrical activity of the left ventricle is characterized by a front propagating through the Purkinje network and then within the heart muscle. In particular, in the normal propagation, the front starts from the atrioventricular (AV) node and propagates in the proximal part of the PF with a velocity in the range 3-4 m/s¹³. At the mid-antero-septal level, located on the endocardium, the PF start to be connected with the ventricular muscle cells through the PMJ. In this way, the electrical signal enters the ventricle muscle and propagates in the whole myocardium, with a reduced conduction velocity in the range 0.3-0.8 m/s¹³.

General overview of the algorithm

The method considered in this work for the generation of a patient-specific Purkinje network has been proposed in (Palamara, Vergara, Faggiano, Nobile, unpublished data, [2013]). The starting point of such a method is the use of a fractal law as proposed in ^{10,11,12}. Then, the generation of the tree has been driven by patient-specific data of the activation times acquired by using an EnSite NavX system. In particular, our method can be summarized in the following steps:

Generation of the patient-specific Purkinje network and computation of the activation times in the ventricle:

- 1) Manually design of the bundle of His and of the main bundle branches;
- 2) Generation of a tentative network without using clinical data;
- 3) Computation of the activation times in the tentative network and in particular at the PMJs;
- 4) Computation of the activation times on the endocardium by using as input the activation times at the tentative PMJs computed at step 3;
- 5) Comparison between the activation times computed at step 4 and the measured data;
- 6) Generation of the patient-specific network as a correction of the tentative one, driven by the discrepancies between computed and measured data obtained at step 5;
- 7) Computation of the activation times in the patient-specific network and in particular at the PMJs;
- 8) Computation of the activation times in the whole ventricle by using as input the activation times at PMJs computed at step 7.

We notice that the algorithm for the patient-specific Purkinje network generation involves only steps from 1 to 6. Here we have added also steps 7 and 8 for the computation of activation times in the whole ventricle since this is the final goal of the PF generation. We also observe that at steps 3-4 and 7-8 we firstly solve the network solely (steps 3,7), and then we use this solution evaluated in the PMJs as sources for the computation of the muscular activation (steps 4,8). This is an explicit solution strategy, since it does not account for the feedback of the muscular activation on the Purkinje network. This choice is justified by the fact that the conduction velocity in the network is greater than that in the myocardium, so that the points of the PF could not be influenced by the muscular propagation. Moreover, we observe that the comparison between computed and measured data at point 5 was performed only on the endocardium, since the measures were available only on such a surface.

Modeling the electrical activity

We illustrate now the mathematical models used to compute the activation times (steps 3,4,7,8 in our algorithm). One of the most widely used models for the description of the electrical activity in the myocardium is the so-called bidomain equation, obtained by considering a propagation both in the extra- and in the intra-cellular spaces^{14,15,16}. However, if one is interested only in the activation times, then the simpler Eikonal equation could be considered^{17,18}. This is a steady model which allows to recover for any point of the computational domain the activation time at which the potential reaches the value $(V_r+V_p)/2$, where V_r is the minimum and V_p the value reached at the plateau.

As observed, the patient-specific clinical data were available only on the endocardium. For this reason, in view of the comparison on step 5 of our algorithm, we needed to know the computed activation times only on the endocardium. Then, we decided to consider the mathematical model for the electrical propagation only on the endocardium (and not in the whole myocardium) given by the isotropic version of the Eikonal model, which reads

$$\begin{aligned} V_e |\nabla u_e| &= 1 \quad \mathbf{x} \in \Omega_e, \\ u_e(\mathbf{x}) &= u_{e,0}(\mathbf{x}) \quad \mathbf{x} \in \Gamma_e, \end{aligned} \quad (1)$$

where $u_e(\mathbf{x})$ is the unknown activation time at a point of the endocardium with coordinates \mathbf{x} , Ω_e is the computational domain, Γ_e is the set of points generating the front, that is the PMJs, $u_{e,0}(\mathbf{x})$ is the value of the activation times in Γ_e , and V_e is the velocity of the front, tuned in the range 0.3-0.8 m/s maximizing the agreement with the clinical measures. We observe that Ω_e is a surface, so that the gradient has to be intended as a the projection of the gradient onto the tangential plane at \mathbf{x} .

For the solution of equation (1) at step 4 of the algorithm, one needs to know the source term $u_{e,0}$ that represents the activation times at the PMJs. To obtain such values, the activation times in the PF tentative network must be known (step 3). Analogously, to compute the final electrical activity in the ventricle (step 8), one needs to know the activation times in the patient-specific network to provide the source terms (step 7). Therefore, we need to introduce a mathematical model to compute the activation times also in a Purkinje network. With this aim, we considered again an isotropic Eikonal model, more precisely

$$\begin{aligned} V_p |\partial u_p / \partial s| &= 1 \quad \mathbf{x} \in \Omega_p, \\ u_p(\mathbf{x}) &= u_{p,0}(\mathbf{x}) \quad \mathbf{x} \in \Gamma_p, \end{aligned} \quad (2)$$

where $u_p(\mathbf{x})$ is the activation time at the point of the network with coordinates \mathbf{x} , Ω_p is the computational domain representing the network, Γ_p is set of points generating the front (for example in the normal case the AV node), $u_{p,0}(\mathbf{x})$ represents the activation times in Γ_p , and V_p is the velocity of the front, supposed to be constant and tuned in the range 3-4 m/s, maximizing the agreement with the clinical measures. We observe that the computational domain Ω_p in this case is a line, so that the derivatives have to be intended as directed along the tangent s .

For the numerical solution of the Eikonal equations (1) and (2) we considered the Fast Marching Method (FMM)¹⁹, implemented in the software VMTK (www.vmtk.org).

Details of the patient-specific generation of the Purkinje fibers network

We provide here a few details of the algorithm described above.

At step 1, the bundle of His and the main bundle branches were manually designed, accordingly to anatomical a priori knowledge^{10,12}. In step 2 a tentative network as a fractal tree was generated. The growing process followed the 'Y' production rule, similar to that implemented in^{10,11,12}, where the number of levels of the tree, the same for each branch, was determined a priori. In our approach, at each level of the generation, we identified active branches and leaves. An active branch can generate other branches, whereas leaves terminate at their end points which are identified with the PMJs. In this way, the branches could be characterized by a different number of levels. To ensure a correct distribution of the PMJs on the endocardium, we described the process of generation of a leaf by means of a Bernoullian probability, where the probability to generate a leaf, p , is a function of the tree level. In particular, p is small for the first levels and grows up for the successive levels. To obtain a more realistic pattern of PF, we described the lengths L_l and L_r and the branching angle α of the new fibers by means of Gaussian variables, with mean value 4.0 ± 0.3 mm for the lengths and $60 \pm 1,8^\circ$ for the angle¹², see Figure 1. The active branches stopped to generate new branches when one or several of the following conditions were satisfied:

- i) The active branches intersected other branches;
- ii) The active branches reached a zone identified either with the base of the ventricle or with the upper areas of the mid-antero septum (both regions being not reached by the Purkinje network²⁰);
- iii) The maximum number of levels defined by the user has been reached.

This procedure allowed to generate a network which in what follows has been referred to as tentative network.

The activation times on the PMJ were then computed by solving the 1D Eikonal equation (2) in the tentative network (step 3). These activation times were then used as sources for the Eikonal problem (1) on the endocardium (step 4), allowing to obtain a tentative activation map which was then compared with the experimental data (step 5).

The algorithm passed then to the final stage, represented by step 6 and consisting in adapting the tentative network to the clinical data. Accordingly, the leaves of the network were moved, added or deleted in order to satisfy the data. This is a completely new step with respect to previous works in the generation of the Purkinje network and allowed to obtain a patient-specific network. In particular, for each point \mathbf{x}_j where the measures were available, we defined the region of influence as the set S_j of PMJs which are possible sources determining the activation time in \mathbf{x}_j when solving a 2D Eikonal equation (1). In other words, the PMJs not belonging to S_j did not contribute in determining the solution in \mathbf{x}_j . Then, the PMJs in S_j were moved, added or deleted in order to minimize the mismatch between the computed and measured activation times in \mathbf{x}_j was minimum. For a detailed description of this step, we refer to (Palamara, Vergara, Faggiano, Nobile, unpublished data, [2013]).

The code for the implementation of our algorithm has been written in C++ using the VTK 5.8 library.

Models for a computational comparison

In order to assess the accuracy of the numerical solutions obtained with our algorithm (referred in what follows to as model D), we compared its performance with that of other three scenarios:

- i) Absence of PF network and localization of a single source for problem (1) at the apex of the ventricle²¹ (model A);
- ii) Absence of the network and localization of the sources for problem (1) driven by the clinical measurements²² (model B). In particular, we prescribed as source points those with the smallest measured activation times;

iii) Presence of the tentative network^{10,11,12} (consisting of only steps 1,2,3,4 of our algorithm, model C).

RESULTS

In this section, we show the numerical results obtained for the two patient described above, referred in what follows as patient 1 and 2. Both cases have undergone to an ablation procedure to eliminate the arrhythmic substrate causing the tachi-arrhythmias. In the first subsection we considered the normal propagation obtained after the therapy, whereas in the second one we considered one unhealthy case before the therapy. The goal is to compare the measured activation times with those computed by the four scenarios considered for the comparison. Given a point on the endocardium where a measure was available, we say that the related datum has been satisfied by one of the four models if the difference in activation time between the datum and the computed value was less than 20%.

Application to cases with normal conduction activity

Our starting points were the geometry reconstructed from the MRI data acquired before the therapy, and the activation times measured after the therapy. We assumed that the geometry did not change as a consequence of the therapy, and we acquired the activation times in 186 points for patient 1 and in 156 for patient 2.

Since we used a probabilistic model to generate the Purkinje networks, each run of our algorithm produced a different outcome. For this reason, we ran the algorithm 20 times, generating 20 tentative and 20 patient-specific networks. In Table 1, first two rows, we reported the mean number and the standard deviation of branches and PMJs in the generated networks. We see that the coefficient of variation (std/mean) is rather small, ranging between 2.5% and 5%. In Figures 2 and 3, bottom, we reported a selected network generated by our algorithm for each case, whereas on the top we indicated the localization of the sources for models A and B.

Then, we solved the Eikonal problem (1) on the endocardium, obtaining the activation times for all the four models, reported in Figures 4 and 5. For models C and D we depicted one selected case over the 20 simulated. The velocities of conduction in the network (V_p) and on the endocardium (V_e) have been tuned in order to maximize the number of satisfied points and it has been kept constant in models C and D. We reported such quantities in Table 1, third and fourth rows. We observe that for models C and D such values fell into the physiological ranges (3-4 m/s for V_p and 0.3-0.8 m/s for V_e). Regarding models A and B, the absence of the PF network has been supplied by choosing a conduction velocity V_e which could change over the domain. In particular, we chose two different values of such a velocity, one in the region of the endocardium which is activated by the PF, and another one in the region characterized by a purely muscular activation (that is at the base of the ventricle and at the upper areas of the mid-antero septum). From Table 1 we observe that for models A and B we let V_e assume values outside the muscular physiological range (but consistent with the conduction velocity in the network) to account for the PF propagation.

In Figures 4 and 5 we also plotted the measured activation times (represented with squares) and the absolute error (that is the distance between computed and measured data) at each point. We observe an excellent qualitative agreement between measured and computed data for models C and D.

In order to quantify the accuracy of the different models, we computed the percentage of satisfied points and the average relative error in activation time between the measures and the prediction by the four models in each measurement point. We reported such values in Table 2, which highlighted the better accuracy when considering a Purkinje network (model C and D) with respect to that obtained without considering a network (models A and B). Moreover, by comparing model A with model B and model C with model D, we observe that the use of clinical measurements to drive the numerical simulations (models B and D) produced better results than those obtained without using any measurements (models A and C).

Application to one case before the ablation therapy

In this section we show the results obtained by applying our algorithm to patient 1 before the ablation procedure. In this case, we acquired the activation times at 179 points on the endocardium. We considered only model D with the assumption that the Purkinje network did not change during the therapy, and a selected network among the 20 generated for the case after the therapy.

Patient 1 was affected by WPW syndrome, that is characterized by an abnormal muscular conduction pathway due to a premature muscular activation. To describe this anomalous propagation, we modeled the premature activation as an additional source in problem (1), located at the points characterized by the lowest measured activation times. We assumed that the anomalous muscular propagation did not activate the PF through the PMJs, so that the network was assumed to be still activated uniquely by the AV node. In such a way, there were two signals propagating: the original one in the PF and the anomalous one through the muscle. Therefore, a muscular site could be activated either by the PMJs as in the normal conduction or by other muscular sites propagating the anomalous signal, depending on which of the two signals arrives earlier. In what follows, we refer to the portion of the Purkinje network which did not activate the muscle due to the presence of the anomalous signal as passive, whereas we refer to the portion of the network which activated the muscle as active. The conduction properties of the network and of the muscle cells were supposed to be the same before and after the therapy, so that we used the same values of V_p and V_e set for the normal case.

In Figure 6 we show the activation maps computed by running steps 7 and 8 in our algorithm, together with the measures depicted with squares. We also drew the active Purkinje network, and we indicated with red bullets the sources of the anomalous propagation and with a blue bullet the mid-antero septum, where the network would have started to interact with the muscle in a normal activation. We observe from the figure in the middle that the anomalous signal propagated from the base towards the apex, that is in the opposite direction with respect to the normal activation.

The agreement between computed and measured data was not so good as for the normal case. In particular, we found that only 21.0% of the points were satisfied, with a mean relative error equal to $176.6 \pm 21.6\%$.

DISCUSSION

Mathematical models of the cardiac electrophysiology allow to compute virtually the electrical activity of the ventricles, providing a non-invasive tool for the study of the pathologies related to the anomalous propagation of the electrical signal⁷. Despite PF have an essential function in the coordinated activation of the ventricles, they have been usually neglected in the computational models²². This was mainly due to the difficulty in obtaining in vivo images of the PF, which are excessively thin for the current clinical imaging resolution.

A common strategy used so far to obtain significant results without generating explicitly the Purkinje network consisted in locating the source of the front at the apex of ventricle (model A)²². An alternative approach has been considered in¹⁹, where the localization of the sources was done by analyzing available clinical data and defining space-dependent conduction properties (model B).

Nevertheless, accounting for the PF in ventricular computational models is essential to simulate not only normal activation, but also pathological cases, such as ventricular dyssynchrony^{8,9}. For this reason, some scientists have attempted to incorporate PF in the mathematical models by their explicit construction. Three possible alternatives have been proposed so far for the latter approach:

- (i) A manual procedure based on anatomical knowledge^{8,23} ;
- (ii) The segmentation of PF from ex vivo images²⁴;
- (iii) The construction of the Purkinje network computationally with a semi-automatic algorithm^{10,11,12}.

In the latter case, the network generation has been driven only by general anatomical information and was not patient-specific (model C). In this work we proposed to use the same approach, where however the construction of PF has been driven by clinical patient-specific data concerning the

activation times on the endocardium (model D). At the best of our knowledge, this has been the first attempt to use clinical data for the explicit construction of the Purkinje network by means of computational tools, allowing to obtain a patient-specific network.

In the first set of simulations we applied the four models to two cases characterized by a normal conduction activity (Figures 2,3,4,5 and Tables 1,2). In such a condition the electrical signal propagates on the endocardium and then into the myocardium starting uniquely from the PMJs. Therefore, the propagation in the myocardium does not influence that on the endocardium. This justified our choice to solve for all the four models a mathematical problem only on the endocardium.

Our results showed that the errors obtained with model B decreased of about 15% in comparisons of those obtained with model A, while the number of satisfied points increased by at least a factor 3. This showed that the use of clinical data could improve the accuracy of the simulations, even without modeling the PF. Errors obtained in model B were however bigger than those obtained when using a Purkinje network, both the tentative and the patient-specific ones (models C and D). In particular, such errors were further reduced of at least 25% with respect to model B, while the number of satisfied points increased of about 25%. This showed the importance of reconstructing the PF (even when no measures were available) to compute the activation times in the ventricle in a normal propagation.

By comparing the performance obtained by using the tentative Purkinje network (model C) with that related to the patient-specific network (model D), we observed that there was a significant improvement in the accuracy when the clinical data were used to drive the network generation. In particular, the errors were reduced by a factor 2, while the number of satisfied points increased by a factor 2. This showed that when clinical measurements are available, it is preferable to generate a patient-specific network, allowing to improve the accuracy.

Regarding the mathematical models used to compute the activation times (problems (1) and (2)), we considered the Eikonal equation both for the PF and for the endocardium. In its more complex version, such equation accounts for the orientation of the muscular fibers and for the diffusion process characterizing the front (anisotropic Eikonal-Diffusion equation^{19,25}). This model was proved to be a good approximation of the more complex bidomain one for computing the activation maps in the myocardium²⁶. In this work, we considered two approximations for this equation. From one hand, we noticed that for a normal activation the signal enters the ventricle at the level of the endocardium, propagating first on such a surface and then in the myocardium. Therefore, the propagation on the endocardium is not influenced by the muscular fibers which are located along the thickness of the myocardium, bringing the signal from the endocardium towards the epicardium. This justified the choice of considering a problem only on the endocardium and then of using the isotropic equation. On the other hand, we neglected the diffusion term, since we assumed that the diffusion process gives a small contribution with respect to the advection one. This was justified by noticing that PF are so dense to inhibit the diffusion to become relevant. Concerning the propagation in the PF, the two approximations were perfectly justified, due to the absence of fibers (and then of anisotropy) in the network, and to the high advection term V_p which dominates any diffusion process.

In the second set of simulations we considered data from patient 1 and we computed the activation times by simulating the abnormal conduction before the ablation procedure (Figure 6). We considered model D solely and we used one of the patient-specific Purkinje network generated from the post-therapy data during the first set of simulations. This was justified by observing that the ablation procedure did not modify the network, since it burned only muscular sites. From Figure 6, we observe that in the region highlighted by the zoom the errors were quite high. In particular, in several points the computed activation time was higher than the measured one. By observing the measures in the septal region (squares in Figure 6, middle) we noticed that the measured signal propagated from the base to the apex. Since in a normal propagation the signal propagates in the opposite direction, we concluded that the anomalous muscular propagation was active in that region. However, from the same figure we observe that the computed activation propagated from the apex to the base, as in the normal case. This means that our algorithm recognized the Purkinje network as active in this region, and this explains the large errors.

The poor accuracy obtained in the septal region in the case before the therapy could be ascribed to the absence of the diffusion term in the 2D Eikonal model and in the solution of a propagation problem only on the endocardium. From one hand, the diffusion process could not be

neglected in the regions activated by the premature muscular activation. Actually, due to the refractility, in such regions the PMJ were off (passive PF network) and the front spread in a region enough wide to make the diffusion processes not negligible. On the other hand, the solution of the propagation only on the endocardium is suitable only for a normal propagation. Indeed, it is known that the premature muscular propagation characterizing the WPW syndrome is due to an anomalous conduction way (the bundle of Kent) which enters the left ventricle in an intramyocardial region, so that in this case the signal reached the endocardium after having propagated through the myocardium, in particular through the muscular fibers. In such a case one needs to account for a 3D Eikonal model with anisotropy, since the muscular fibers influence the propagation on the endocardium. This is currently under study and it will be the subject of future works.

The main contributions of the present work are summarized in what follows:

- We showed, for the first time, the feasibility of using clinical measurements of the activation times on the endocardium to drive the Purkinje network generation by means of computational tools, allowing to recover patient-specific networks;
- We showed the importance of generating a Purkinje network to recover an accurate electrical activation on the endocardium for a normal propagation;
- We showed the improvements in the accuracy in the case of a normal propagation when patient-specific measures were used to generate the network;
- We showed that the simple isotropic Eikonal model solved only on the endocardium was enough to describe the normal propagation on such a surface, whereas we believe that the 3D anisotropic Eikonal-Diffusion equation should be used in presence of an anomalous muscular propagation.

SOURCES OF FUNDING

The present study has been funded by Fondazione Cassa di Risparmio di Trento e Rovereto (CARITRO) within the project "Numerical modelling of the electrical activity of the heart for the study of the ventricular dissincrony".

DISCLOSURES

None.

REFERENCES

1. Durrer D, van Dam RT, Freud GE, Janse MJ, Meijler FL, Arzbaecher RC. Total excitation of the isolated human heart. *Circulation*. 1970;41(6):899-912.
2. Scheinman MM. Role of the His-Purkinje system in the genesis of cardiac arrhythmia. *Heart Rhythm*. 2009;6(7):1050-1058.
3. Catanzariti D, Maines M, Manica A, Angheben C, Varbaro A, Vergara G. Permanent His-bundle pacing maintains long-term ventricular synchrony and left ventricular performance, unlike conventional right ventricular apical pacing. *Europace*. 2006; doi:10.1093/europace/eus313.
4. Catanzariti D, Maines M, Cemin C, Broso G, Marotta T, Vergara G. Permanent direct his bundle pacing does not induce ventricular dyssynchrony unlike conventional right ventricular apical pacing. An inpatient acute comparison study. *J Interv Card Electrophysiol* . 2012;16:81–92.

5. Rawling DA, Joyner RW, Overholt ED. Variations in the functional electrical coupling between the subendocardial purkinje and ventricular layers of the canine left ventricle. *Circ Res.* 1985;57(2):252-261.
6. Anderson RH, Yanni J, Boyett MR, Chandler NJ, Dobrzynski H. The anatomy of the cardiac conduction system. *Clin Anat.* 2009;22(1):99-113.
7. Keener J, Sneyd J. *Mathematical Physiology.* New York, Springer; 1998.
8. Tusscher KH, Panfilov AV. Modelling of the ventricular conduction system. *Prog Biophys Mol Biol.* 2008;96(1-3):152-170.
9. Romero D, Sebastian R, Bijnens B, Zimmerman V, Boyle P, Vigmond E, Frangi A. Effects of the Purkinje system and cardiac geometry on biventricular pacing: A model study. *Ann Biomed Eng.* 2010;38:1388-1398.
10. Abboud S, Berenfeld O, Sadeh D. Simulation of high-resolution qrs complex using a ventricular model with a fractal conduction system. Effects of ischemia on high-frequency qrs potentials. *Circ Res.* 1991;68(6):1751-1760.
11. Ijiri T, Ashihara T, Yamaguchi T, Takayama K, Igarashi T, Shimada T, Namba T, Haraguchi R, Nakazawa K. A procedural method for modeling the Purkinje fibers of the heart. *J Physiol Sci.* 2008; 58(7):481-486.
12. Sebastian R, Zimmerman V, Romero D, Frangi AF. Construction of a computational anatomical model of the peripheral cardiac conduction system. *IEEE T Biomed Eng.* 2011;58(12):3479-3482.
13. Kerckhoffs RC, Faris OP, Bovendeerd PH, Prinzen FW, Smits K, McVeigh ER, Arts T. Timing of depolarization and contraction in the paced canine left ventricle: model and experiment. *J Cardiovasc Electr.* 2003;14(10 Suppl):S188-S195.
14. Keener JP, Bogar K. A numerical method for the solution of the bidomain equations in cardiac tissue. *Chaos.* 1998;8(1):234-241.
15. Vigmond EJ, Aguel F, Trayanova NA. Computational techniques for solving the bidomain equations in three dimensions. *IEEE Trans Biomed Eng.* 2002;49(11):1260-1269.
16. Colli Franzone P, Pavarino LF. A parallel solver for reaction–diffusion systems in computational electrocardiology. *Math Models Methods Appl.* 2004;14(06):883-911.
17. Keener JP. An eikonal-curvature equation for action potential propagation in myocardium. *J Math Biol.* 1991;29(7):629-651.
18. Colli Franzone P, Guerri L. Spreading excitation in 3-D models of the anisotropic cardiac tissue, I. Validation of the Eikonal Model, *Math Biosci.* 1993;113:145-209.
19. Sethian JA. *Level Set Methods and Fast Marching Methods: Evolving Interfaces in Computational Geometry, Fluid Mechanics, Computer Vision, and Materials Science.* Cambridge, Cambridge University Press; 1999.
20. Sebastian R, Zimmerman V, Romero D, Sanchez-Quintana D, Frangi A. Characterization and Modeling of the Peripheral Cardiac Conduction System. *IEEE T Med Imaging.* 2012; in press. DOI: 10.1109/TMI.2012.2221474.
21. Rodriguez B, Li L, Eason JC, Efimov IR, Trayanova NA, Differences between left and right ventricular chamber geometry affect cardiac vulnerability to electric shocks. *Circ Res.* 2005;97(2):168-175.
22. Sermesant M, Chabiniok R, Chinchapatnam P, Mansi T, Billet F, Moireau P, Peyrat JM, Wong K, Relan J, Rhode K, Ginks M, Lambiase P, Delingette H, Sorine M, Rinaldi CA, Chapelle D, Razavi R, Ayache N. Patient-specific electromechanical models of the heart for the prediction of pacing acute effects in CRT: a preliminary clinical validation. *Med Image Anal.* 2012;16(1):201-215.
23. Berenfeld O, Jalife J. Purkinje-muscle reentry as a mechanism of polymorphic ventricular arrhythmias in a 3-dimensional model of the ventricles. *Circ Res.* 1998;82(10):1063-1077.
24. Bordas R, Gillow K, Lou Q, Efimov IR, Gavaghan D, Kohl P, Grau V, Rodriguez B. Rabbit-specific ventricular model of cardiac electrophysiological function including specialized conduction system. *Prog Biophys Mol Biol,* 2011;107(1):90-100.
25. Pashaei A, Romero D, Sebastian R, Camara O, Frangi AF. Fast multiscale modeling of cardiac electrophysiology including purkinje system. *IEEE T Biomed Eng.* 2011;58(10):2956-2960.

26. Colli Franzone P, Guerri L, Pennacchio M, Taccardi B. Spread of excitation in 3-d models of the anisotropic cardiac tissue. II. Effects of fiber architecture and ventricular geometry. *Math Biosci.*1998; 147(2):131-171.

TABLES

		model A	model B	model C	model D
patient 1	# branches	X	X	1977±42	1724±46
	# PMJ	X	X	494±13	239±10
	V_p (m/s)	X	X	3.92	3.92
	V_e (m/s)	2.4/0.8	2.4/0.8	0.65	0.65
patient 2	# branches	X	X	1382±30	1218±51
	# PMJ	X	X	343±12	179±39
	V_p (m/s)	X	X	3.94	3.94
	V_e (m/s)	2.4/0.8	2.4/0.8	0.65	0.65

Table 1. Number of branches and of PMJ of the networks generated by our algorithm (models C and D), and estimated conduction velocities in the network (V_p) and on the endocardium (V_e). For V_e in models A and B the first value refers to the endocardium excluding the base of the ventricle and the upper areas of the septum, while the second one refers to the base of the ventricle and the upper areas of the mid-antero septum. For models C and D the results have to be intended as the average over the 20 simulations

	PATIENT 1				PATIENT 2			
	model A	model B	model C	model D	model A	model B	model C	model D
satisfied points (%)	11.2	32.8	39.9±2.3	66.7±1.5	1.6	20.8	25.3±3.9	63.1±2.4
mean relative error (%)	50.0±5.5	43.0±6.3	33.9±6.8	19.9±5.3	83.8±12.4	75.5±9.0	63.9±8.6	28.6±6.0

Table 2. Percentage of satisfied points (that is characterized by an error less than 20%) and mean relative error for both patients in the four scenarios. Normal activation. For models C and D the results have to be intended as the average over the 20 simulations

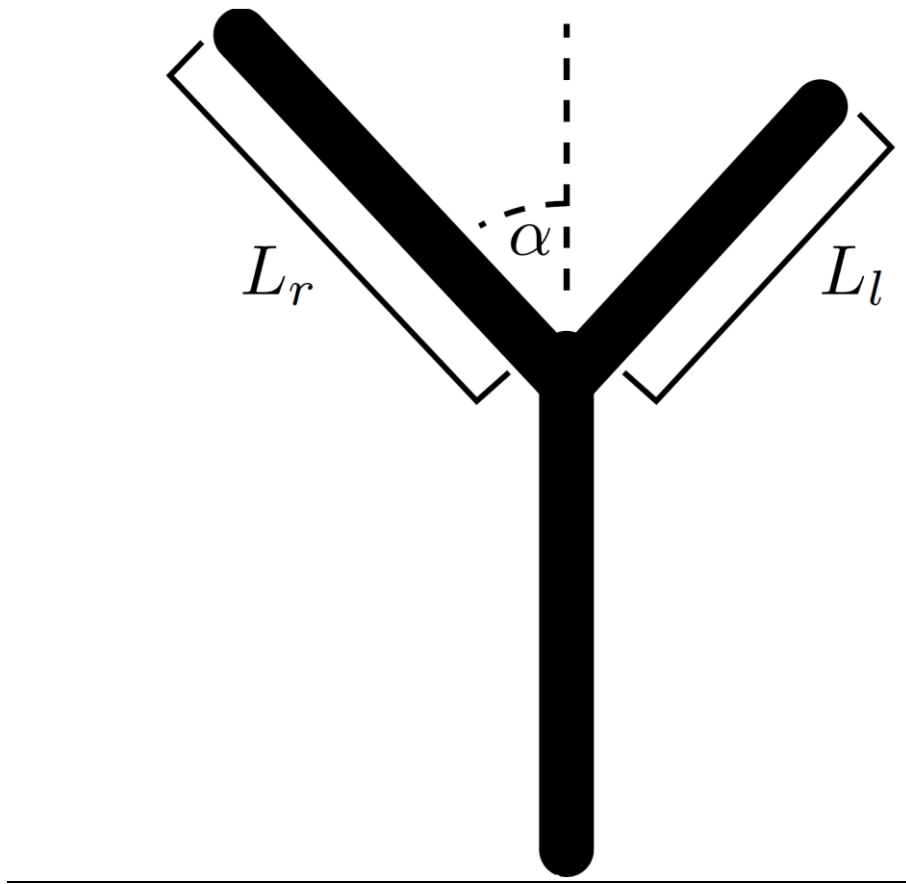


Figure 1. Schematic representation of the generation of two new branches in the Purkinje network. L_l , L_r and α indicate Gaussian variables.

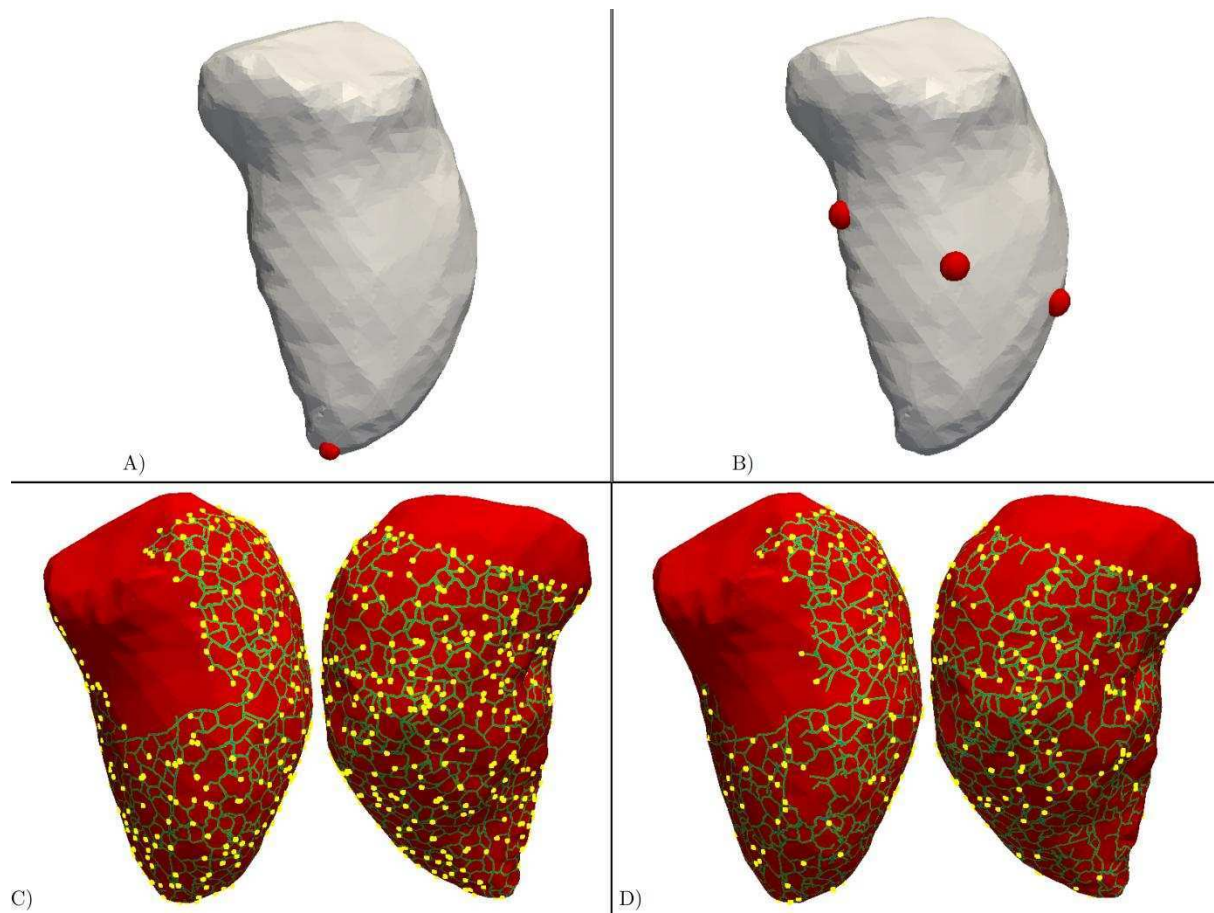


Figure 2. Top. Localization of the sources in the models without PF: Model A (left) and model B (right). Bottom. Tentative (model C, left) and patient-specific (model D, right) Purkinje networks generated by our algorithm. In yellow we depicted the PMJ. For models C and D we depicted one selected case over the 20 simulated. Patient 1.

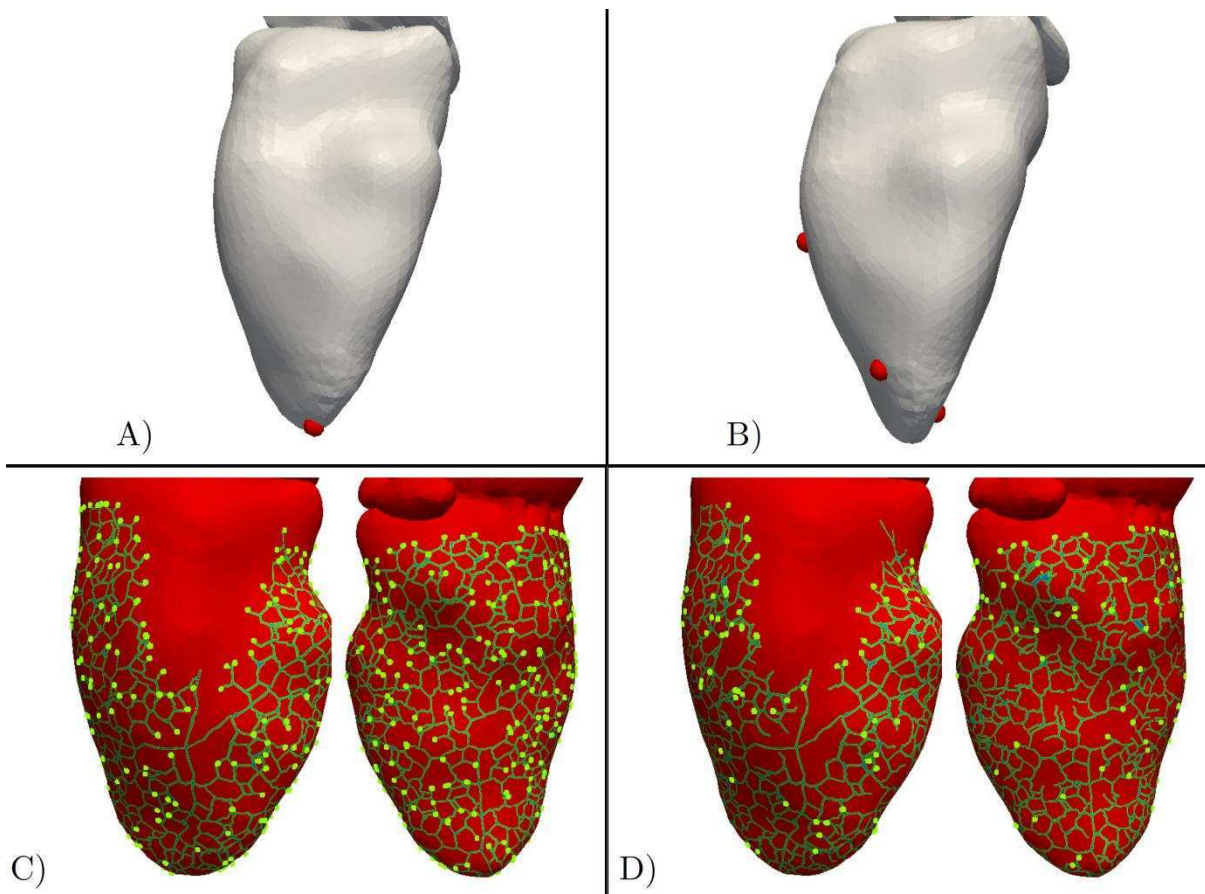


Figure 3. Top. Localization of the sources in the models without PF: Model A (left) and model B (right). Bottom. Tentative (model C, left) and patient-specific (model D, right) Purkinje networks generated by our algorithm. In yellow we depicted the PMJ. For models C and D we depicted one selected case over the 20 simulated. Patient 2.

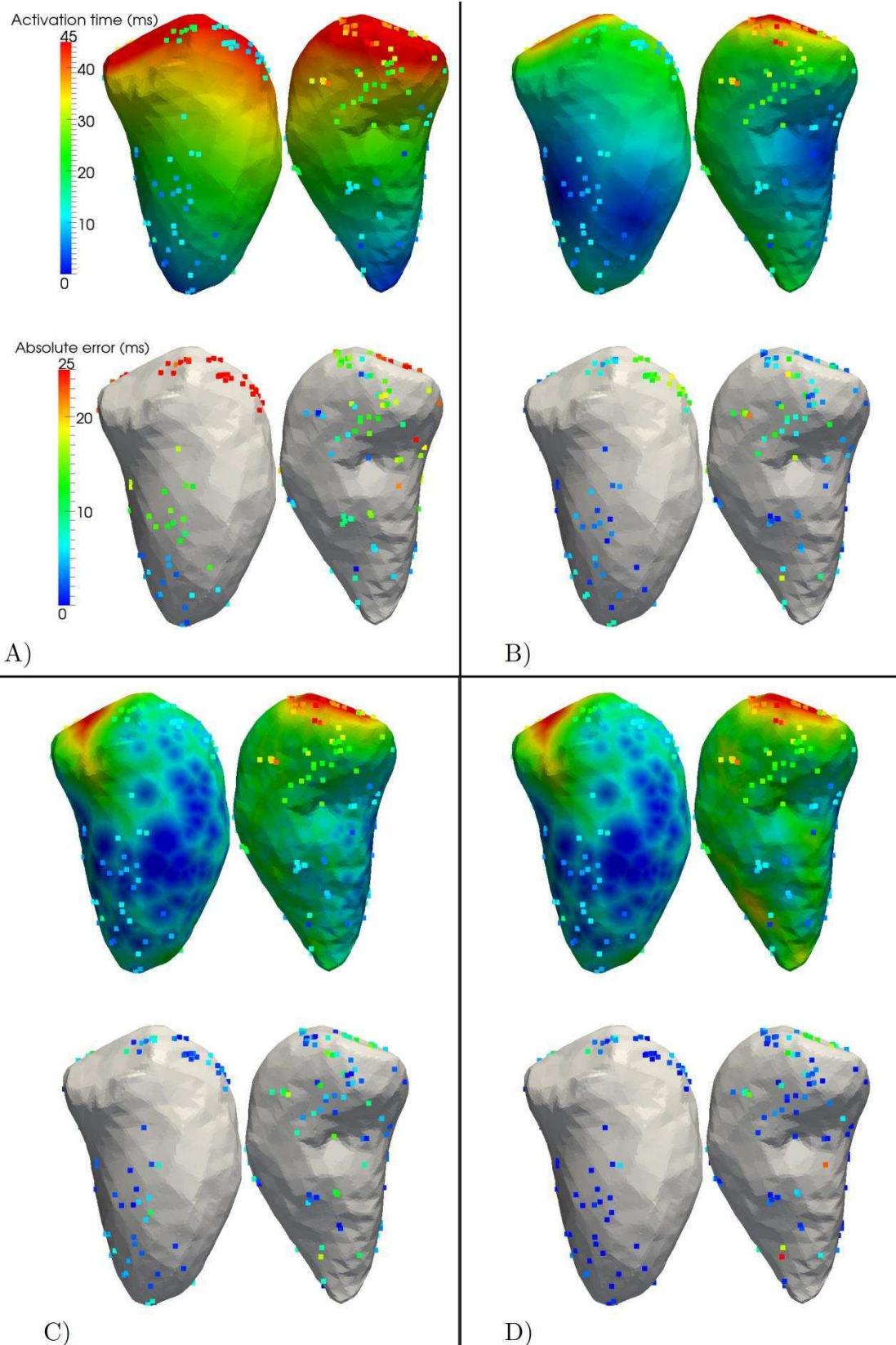


Figure 4. Computed activation times and errors for the four models. Top left, model A. Top right, model B. Bottom left, model C. Bottom right, model D. For each case, in the upper row we depicted the computed activation times (the measured data are plotted with squares), and in the lower row we represented the absolute errors. For models C and D we depicted one selected case over the 20 simulated. Patient 1, normal activation.

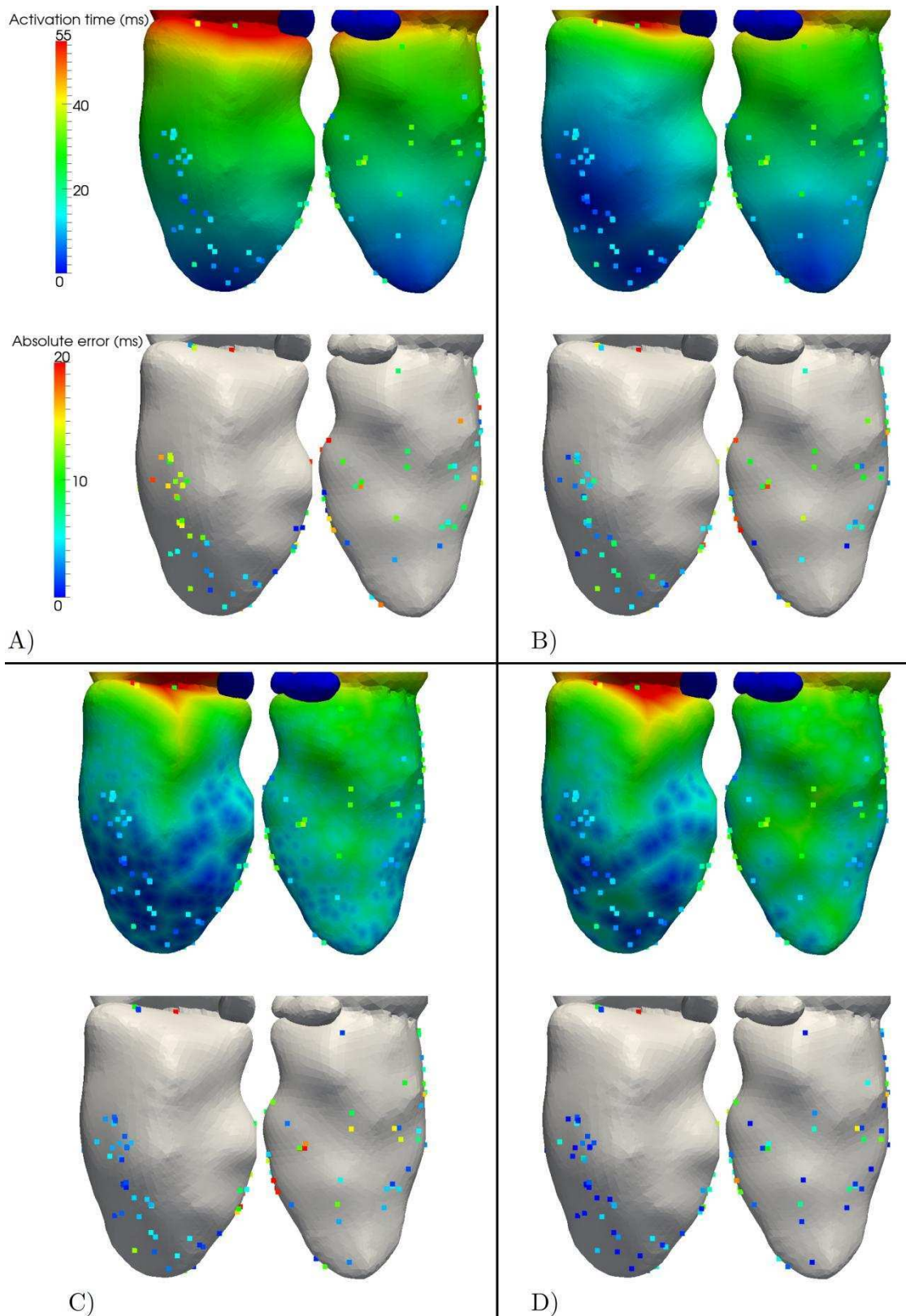


Figure 5. Computed activation times and errors for the four scenarios. Top left, model A. Top right, model B. Bottom left, model C. Bottom right, model D. For each case, in the upper row we depicted the computed activation times (the measured data are plotted with squares), while in the lower row we represented the absolute errors. For models C and D we depicted one selected case over the 20 simulated. Patient 2, normal activation.

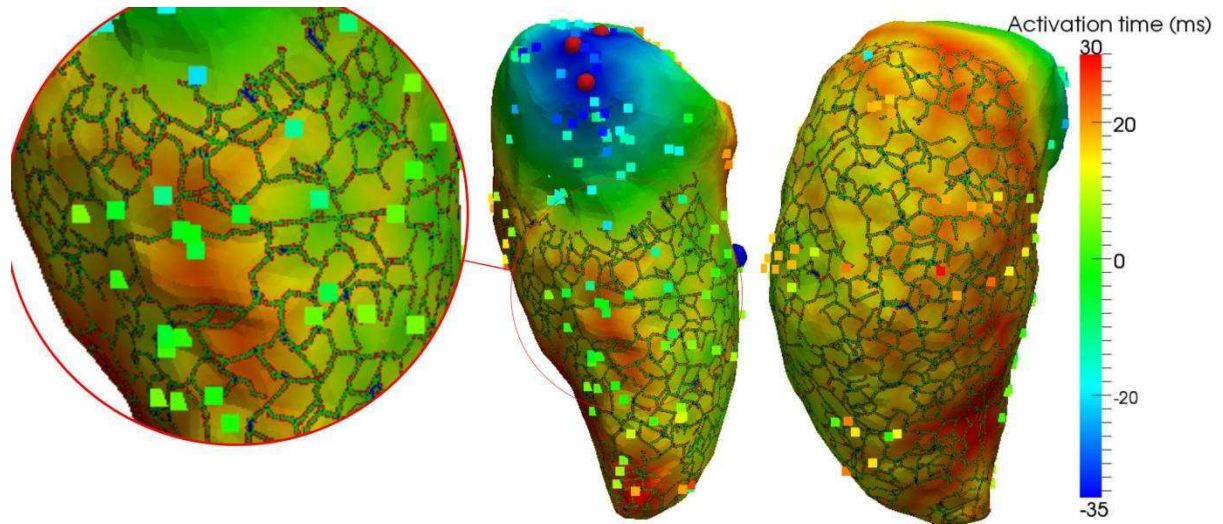


Figure 6. Computed activation times for model D before the ablation procedure. The measured data are plotted in square. We drew only the active PF network. The red bullets represents the sources of the anomalous signal, whereas the blue one the mid-antero-septal region, i.e. where the network starts to interact with the muscle for a normal propagation. The origin of the time scale has been set accordingly to the case after the therapy. Patient 1, activation characterized by the WPW syndrome.

MOX Technical Reports, last issues

Dipartimento di Matematica “F. Brioschi”,
Politecnico di Milano, Via Bonardi 9 - 20133 Milano (Italy)

- 09/2013** VERGARA, C.; PALAMARA, S.; CATANZARITI, D.; PANGRAZZI, C.; NOBILE, F.; CENTONZE, M.; FAGGIANO, E.; MAINES, M.; QUARTERONI, A.; VERGARA, G.
Patient-specific computational generation of the Purkinje network driven by clinical measurements
- 08/2013** CHEN, P.; QUARTERONI, A.; ROZZA, G.
A Weighted Reduced Basis Method for Elliptic Partial Differential Equations with Random Input Data
- 07/2013** CHEN, P.; QUARTERONI, A.; ROZZA, G.
A Weighted Empirical Interpolation Method: A-priori Convergence Analysis and Applications
- 06/2013** DED, L.; QUARTERONI, A.
Isogeometric Analysis for second order Partial Differential Equations on surfaces
- 05/2013** CAPUTO, M.; CHIASTRA, C.; CIANCIOLO, C.; CUTRI, E.; DUBINI, G.; GUNN, J.; KELLER, B.; ZUNINO, P.;
Simulation of oxygen transfer in stented arteries and correlation with in-stent restenosis
- 04/2013** MORLACCHI, S.; CHIASTRA, C.; CUTR, E.; ZUNINO, P.; BURZOTTA, F.; FORMAGGIA, L.; DUBINI, G.; MIGLIAVACCA, F.
Stent deformation, physical stress, and drug elution obtained with provisional stenting, conventional culotte and Tryton-based culotte to treat bifurcations: a virtual simulation study
- 03/2013** ANTONIETTI, P.F.; AYUSO DE DIOS, B.; BERTOLUZZA, S.; PENNACCHIO, M.
Substructuring preconditioners for an $h - p$ Nitsche-type method
- 02/2013** BRUGIAPAGLIA, S.; GEMIGNANI, L.
On the simultaneous refinement of the zeros of H -palindromic polynomials
- 01/2013** ARNOLD, D.N.; BOFFI, D.; BONIZZONI, F.
Tensor product finite element differential forms and their approximation properties

56/2012 IEVA, F.; PAGANONI, A.M.
*Risk Prediction for Myocardial Infarction via Generalized Functional
Regression Models*